Met. Mater. Int., Vol. 23, No. 4 (2017), pp. 805~812
doi: 10.1007/s12540-017-6869-4

Tensile Property Improvement in Ti/Al Clad Sheets Fabricated by Twin-Roll Casting and Annealing

Dong Ho Lee, Jung-Su Kim, Hyejin Song, and Sunghak Lee*

Center for Advanced Aerospace Materials
Pohang University of Science and Technology, Pohang 37673, Republic of Korea

(received date: 2 December 2016 / accepted date: 12 December 2016)

A new fabrication method of Ti/Al clad sheet by bonding a thin Ti sheet on to Al alloy melt during twin-roll casting was presented to broaden industrial applications of Ti alloys. In the twin-roll-cast Ti/Al clad sheet, a homogeneously solidified microstructure existed in the cast Al side, while a Ti/Al interface did not contain pores, cracks, or lateral delamination, which indicated a successful fabrication. When this cast sheet was annealed at 400 °C, metallurgical bonding was expanded by interfacial diffusion, thereby leading to improvement in tensile properties. After the 600 °C-annealing, a $TiAl_3$ intermetallic compound was formed at the Ti/Al interface, which deteriorated tensile properties because of its brittle characteristics. The yield and tensile strengths of the 400 °C-30-min-annealed sheet (132 MPa and 218 MPa, respectively) were higher than those (103 MPa and 203 MPa, respectively) calculated by a rule of mixtures using tensile properties of a 5052-O Al alloy and a pure Ti. Its ductility was also higher than that of 5052-O Al alloy (25%) or pure Ti (25%) because the strain at the interfacial delamination point reached 41%. The 400 °C-30-min-annealed sheet showed the overall homogenous deformation behavior by complimenting drawbacks of mono-layer of Al or Ti.

Keywords: vertical twin-roll casting, Ti/Al clad sheet, annealing, interfaces, intermetallics

1. INTRODUCTION

Ti alloys have many advantages such as excellent strength-to-density ratio, resistance to corrosion and oxidation, and high-temperature properties [1-8]. However, wide applications of Ti alloys to various industries have been limited because of their shortcomings such as poor formability and expensiveness. In order to broaden their applications, many efforts have been dedicated to manufacture thin Ti alloy sheets clad with other alloys such as inexpensive and readily formable Al alloys or stainless steels by direct solid/solid-state bonding methods. Since these methods are usually proceeded under high temperatures and reduction ratios, the interfacial bonding is often deteriorated by forming brittle interfacial layers composed of intermetallic compounds [9-16]. As a promising approach for liquid/solid-state bonding, twin-roll casting, which is a method to continuously cast thin strips right after melting of objective alloys, has been recently suggested [17]. The rapid solidification of twin-roll casting, compared to conventional continuous casting, can be exploited as an environmentally conscious production process for refining solidification structure and reducing micro-segregation [18-23]. If the fabrication method of Ti/Al clad sheets by utilizing advantages of twin-roll casting and by cladding thin Ti sheet on to the twin-roll-cast Al alloy melt can be developed, thus, the inherent shortcomings of Ti alloys can be solved.

Very few studies have been made on the solidification of substrate alloy (Al alloy) and interfacial bonding of Ti during the twin-roll casting [24-26]. Since the solidification proceeds under a direct contact of a roll with a solidified Al alloy melt shell and a thin Ti sheet, different approaches and solutions for excellent liquid/solid-state bonding are required. After the successful twin-roll casting, the interfacial bonding of twin-roll-cast Ti/Al clad sheets should be further improved because it is not enough to be strongly bonded. Interfacial bonding should be optimally controlled, but effects of microstructural and process parameters on interfacial bonding have not been sufficiently investigated [27]. In the present study, therefore, Ti/Al clad sheets were fabricated by twin-roll casting followed by annealing to achieve an economical cladding method. Microstructures of fabricated clad sheets were analyzed, and their properties were evaluated by conducting tensile tests. This fabrication involving concepts of twin-roll casting and annealing would be useful because production costs of Ti/Al clad sheets can be reduced.

*Corresponding author: shlee@postech.ac.kr

2. EXPERIMENTAL PROCEDURE

2.1. Twin-roll casting of Ti/Al clad sheet

A 5052 Al alloy (composition; Al-0.25Si-0.40Fe-0.10Cu-0.10Mn-(2.2-2.8)Mg-0.10Zn-(0.15-0.35)Cr (wt%)) was subjected to vertical twin-roll casting. Figure 1 schematically illustrates a vertical twin-roll caster composed of tundish (diameter; 72 mmφ, depth; 60 mm), crucible, twin rolls (diameter; 400 mmφ, length; 200 mm, torque; 15 hp), Ti-sheet uncoiler, and brusher. The 5052 Al alloy was induction-melted at 680 °C in a crucible, and the amount of Al alloy melt was controlled by a stopper. The alloy melt was transferred into a tundish, and then was twin-roll-cast with a thin pure Ti sheet (thickness; 0.5 mm, width; 68 mm) to fabricate 3.0-mm-thick two-ply Ti/Al clad sheets. The Ti sheet was uncoiled by an uncoiler, and its surface was mechanically deoxidized by a brusher.

In the fabrication of Ti/Al clad sheets, the Al melt was directly contacted with Ti sheet and Cu-faced rolls whose thermal conductivity was much higher than the Ti sheet. Since the sufficient solidification of Al melt might be difficult, large-diameter twin rolls having water-circulating cooling system were used. The temperature of Al melt was kept as low as possible by using a cooling slope [22], and the time for contacting the Al melt with the Ti sheet was extended by reducing the roll speed and roll gap so as to achieve the sufficient solidification of Al melt. Another objective of the low-temperature Al melt is to prevent the formation of Ti-Al-based intermetallic compounds at the Ti/Al interface, whose formation temperatures are about 600 °C [11-14,27-29]. The roll gap and speed were set at 3.0 mm and 30 mm/s (4.4 rpm), respectively. When the Al melt temperature was too low or the roll speed was too slow, the Al melt was rapidly solidified before passing through twin rolls. In the opposite cases, the cast strip or Ti sheet was overheated, and its surface was locally molten or inhomogeneously roughened by a contraction of the Al melt.

The twin-roll-cast Ti/Al clad sheets were annealed at 400 °C for 10-30 min for the stress relief of the cast 5052 Al substrate. This annealing was used to simulate an actual O-temper treatment (annealing at 345-415 °C) of commercial 5052 Al alloys [30]. They were also annealed at 600 °C for 10-30 min to investigate effects of formation of interfacial intermetallic compounds on tensile properties because some Ti-Al-based intermetallic compounds are formed around 600 °C and are grown with increasing annealing time. For convenience, the as-twin-roll-cast sheet is designated as 'AS', and the sheets annealed at 400 °C or 600 °C for 10 min and 30 min are referred to as 'A41', 'A43', 'A61', and 'A63', respectively.

2.2. Microstructural analyses and tensile tests

These Ti/Al clad sheets were sectioned and mechanically polished with a diamond paste (size; 1 μm) before observing microstructures of longitudinal-short-transverse (L-S) plane by an optical microscope and a scanning electron microscope

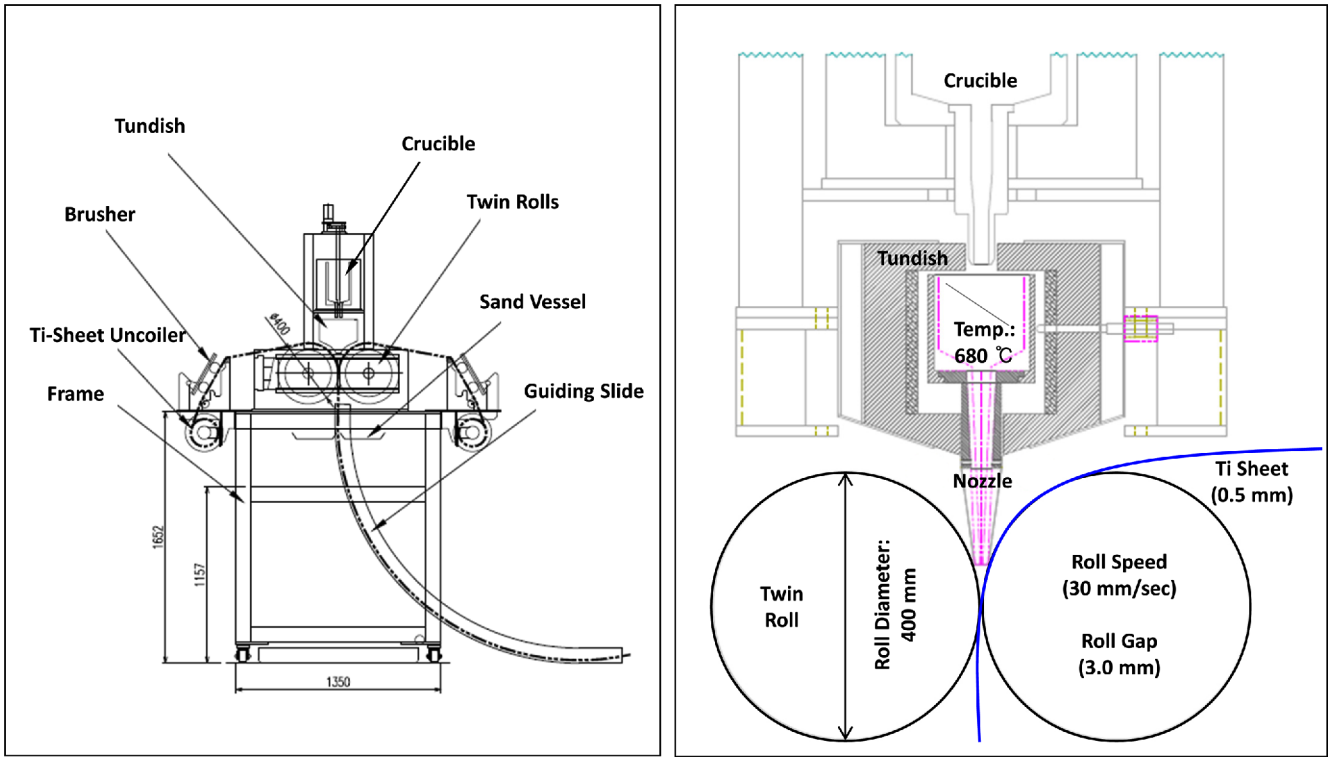

Fig. 1. Schematic diagrams of a vertical twin-roll caster composed of tundish, crucible, stopper, twin rolls, guide rolls, Al-sheet uncoiler, and brusher.

(SEM, model; JSM-6330F, JEOL, Japan). Phases existed in the Ti/Al interface were analyzed by an energy dispersive spectroscopy (EDS).

Plate-type tensile specimens (gage length; 20.0 mm, gage width; 5.0 mm, gage thickness; 3.0 mm) were prepared in the longitudinal direction. They were tested at room temperature at a strain rate of 10^{-3} s^{-1} by a universal testing machine (model; Instron 1361, Instron Corp., Canton, MA, USA) of 100 kN capacity, in accordance with ASTM E 8/E 8M standard specification [31].

2.3. Digital imaging strain analysis

Digital image correlation (DIC) is a basic technique to measure the deformation amount including localized deformation strain during the tensile test [32,33]. Photographs of the tensile specimen surface were taken by two cameras (model: Phantom V7.3, Komi, Korea), and a vision strain gauge system (model; ARAMIS 5M, GOM Optical Measuring Techniques, Germany) was used for detecting 3-dimensional coordinates of a deforming specimen surface. High-quality white- and black-color lacquers (model: Aqua, Motip Dupli, Germany) were sprayed on the longitudinal-transverse (L-T) plane of the tensile specimen to obtain random black-and-white speckled patterns, which were then used for the strain distribution analysis. This system recognized the surface structure in digital camera images, and allocated coordinates to image pixels. The first image in the measuring specimen represented the undeformed state, and further images were recorded during the deformation. The nominal and local strains at the position from the base line (the center of the gage section) were measured along the center line of the gage section by comparing the digital images.

3. RESULTS

3.1. Microstructures of twin-roll-cast Ti/Al clad sheets

Figure 2(a) is a low-magnification optical photograph showing a side view of an as-twin-roll-cast clad sheet (AS sheet) fabricated by optimal parameters (melting temperature of Al alloy; 680 °C, roll speed; 30 mm/s, roll gap; 3.0 mm, Ti sheet thickness; 0.5 mm). The cast structure is relatively homogeneously formed in the Al alloy substrate side, while wrinkles are not formed in the Ti side in spite of the difference in thermal conductivity of Ti and Al [34]. A Ti/Al interface is clearly observed, but does not contain any pores, cracks, or lateral delamination. The thickness of the AS sheet is 3.0 mm, and that of the Ti layer (0.5 mm) is hardly reduced because the Ti sheet was not molten during the twin-roll casting. When the Ti/Al interface is observed in a compo-image (made by detection of secondary and back-scattered electrons) inside an SEM (Fig. 2(b)), the cast Al structure is relatively homogeneous, and any reaction products are hardly observed, which indicates the successful fabrication of the Ti/Al clad sheet.

SEM micrographs of the cross-sectional area of the Ti/Al clad sheets annealed at 400 °C or 600 °C are shown in Figs. 3(a) through 3(d). After the 400 °C-annealing for 10 min or 30 min, the basic microstructures are hardly changed, while residual stresses formed during the twin-roll casting might be reduced or removed (Figs. 3(a) and 3(b)). After the 600 °C-annealing for 10 min, a thin interfacial layer (thickness; 1.2 μm) is observed as shown in Fig. 3(c), and is thickened to 2.9 μm as the annealing time increases (Fig. 3(d)). A high-magnification SEM micrograph of the A63 sheet is shown in Fig. 4(a). A reaction layer is observed along the Ti/Al interface. From an EDS composition profile of Ti and Al (Fig. 4(b)), the reaction layer is identified to be $TiAl_3$ phase, which is a characteristic intermetallic compound given in the Ti-Al phase diagram [35], as marked by an arrow in Fig. 4(a). The $TiAl_3$ phase is known to be formed at about 600 °C which is far lower than the formation temperatures of TiAl or Ti_3Al phase [13].

3.2. Room-temperature tensile properties

Figures 5(a) through 5(c) show engineering tensile stress-strain curves of the AS, A41, A43, A61, and A63 sheets, from which the yield strength, ultimate tensile strength, and elongation are measured, as shown in Table 1. The AS sheet shows

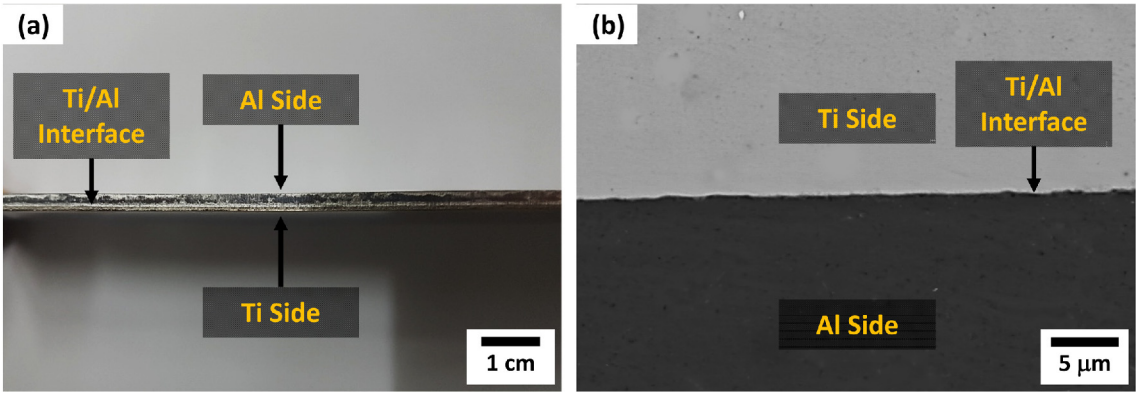

Fig. 2. Side-view optical photograph and a compo-image SEM micrograph showing a Ti/Al interface of a twin-roll-cast Ti/Al clad sheet fabricated by optimal process parameters (melting temperature of Al alloy; 680 °C, roll speed; 30 mm/s, roll gap; 3.0 mm, Ti sheet thickness; 0.5 mm).

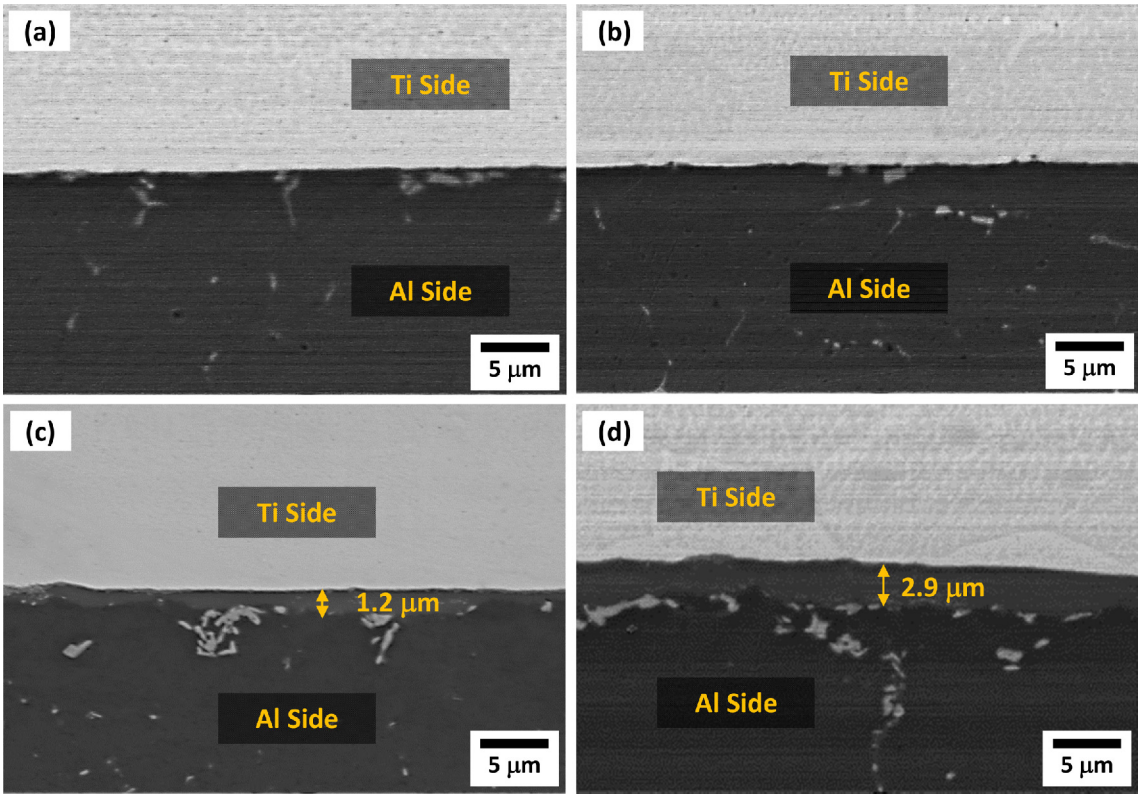

Fig. 3. SEM micrographs of the cross-sectional area of the Ti/Al clad sheets annealed at (a) and (b) 400 °C and (c) and (d) 600 °C. After the 600 °C-annealing for 10 min, a thin interfacial layer (thickness; 1.2 μm) is formed, and is thickened to 2.9 μm as the annealing time increases.

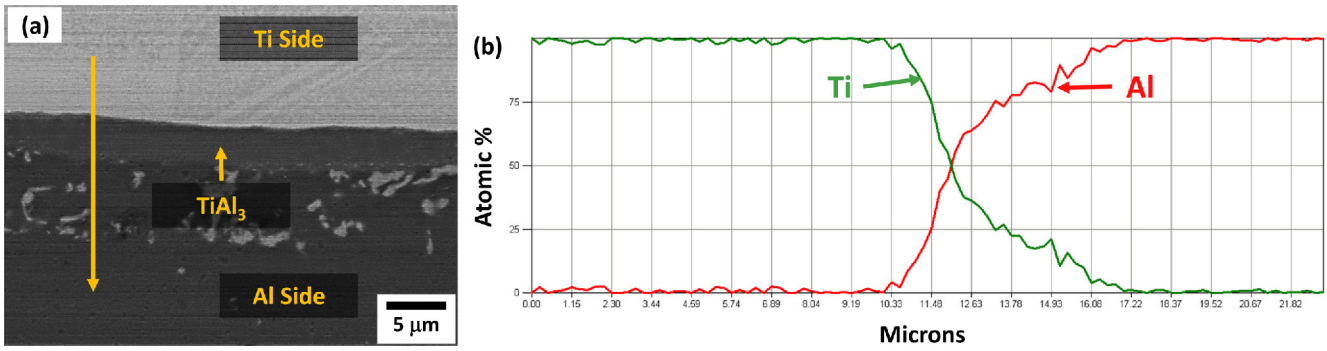

Fig. 4. (a) High-magnification SEM micrograph and (b) EDS composition profile of Ti and Al of the A63 sheet. An interfacial reaction layer is identified to be $TiAl_3$ phase, which is a characteristic intermetallic compound given in the Ti-Al phase diagram [35].

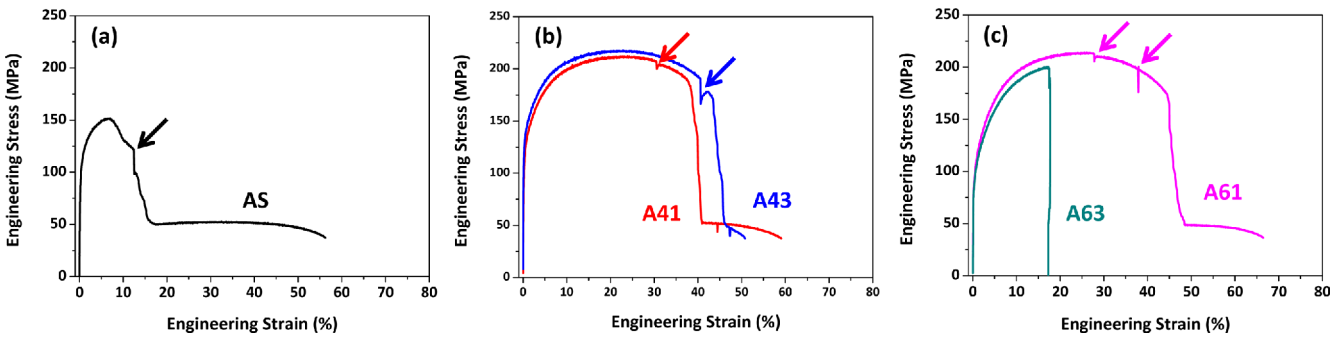

Fig. 5. Room-temperature engineering tensile stress-strain curves of the (a) AS, (b) A41 and A43, and (c) A61 and A63 sheets. Some rapid stress drops are observed in the stress-strain curves.

Table 1. Room-temperature tensile properties of the twin-roll-cast Ti/Al clad sheets

Clad Sheet	Yield Strength (MPa)	Tensile Strength (MPa)	Total Elongation (%)	Strain at Interfacial Delamination (%)
AS	99 ± 5	152 ± 7	17.0 ± 1.2	12.5 ± 0.8
A41	118 ± 7	211 ± 7	41.1 ± 0.8	30.6 ± 0.8
A43	132 ± 5	218 ± 9	50.2 ± 1.8	40.5 ± 1.5
A61	91 ± 3	214 ± 5	48.8 ± 1.1	27.9 ± 1.1
A63	83 ± 3	198 ± 3	17.4 ± 2.1	17.2 ± 0.5

the lowest strength and elongation with a little plastic range (Fig. 5(a)). The A41 and A43 sheets have much higher strength and elongation than the AS sheet (Fig. 5(b)). The A61 sheet shows similar tensile properties to those of the A41 and A43 sheets, but the elongation of the A63 sheet is seriously deteriorated (Fig. 5(c)). Some rapid stress drops are observed in the stress-strain curves of all the Ti/Al clad sheets as marked by arrows.

3.3. Tensile flow behavior – Digital image correlation (DIC)

In order to investigate the detailed deformation behavior including rapid stress drops, which can be hardly observed or clarified during the tensile tests, the vision strain gauge system was simultaneously used with the tensile test. Figures 6(a) through 6(d) show digital images of strain distribution of the tensioned Ti/Al clad sheets. These digital image data can be collected from several hundreds of high-resolution images. In the AS sheet, seven digital images of strain distribution in the strain range from 2% to fracture strain are selected, as shown in Fig. 6(a). The AS sheet is rapidly cracked in the Al side as soon as the tensile deformation starts, and the crack is blunted and grown into the interior. At the strain of 13%, the Ti/Al interface is delaminated, which leads to the rapid stress drop in the stress-strain curve (Fig. 5(a)). When the AS sheet is further tensioned, the sheet specimen is fractured as the crack is connected with the delaminated Ti/Al interface. The necking is hardly observed in this specimen.

The A41 sheet is homogeneously deformed in the strain range of 5%-20%, and the necking starts at the strain of 25% (Fig. 6(b)). After the necking, the tensile deformation is concentrated to reach the maximum local strain of about 40%. At the strain of 31%, the Ti/Al interfacial delamination occurs, which is also matched with the stress drop in Fig. 5(b). After the interfacial delamination, the Al substrate is tensioned further to reach the fracture strain (41%). The A43 sheet shows almost similar tensile deformation behavior to the A41 sheet (Fig. 6(c)). The necking and interfacial delamination occur at the strains of 30% and 41%, respectively, which are higher than those of the A41 sheet. In the A61 sheet, the necking starts at the strain of 20%, the deformation is concentrated in a shear mode in a relatively wide area (Fig. 6(d)), which is somewhat different from the deformation mode of the A41 or A43 sheet. The interfacial delamination firstly occurs at the strain of 28%, which are lower than that of the A41 or A43 sheet. After the first interfacial delamination, the A61 sheet is deformed further to the strain of 38%, at which the second interfacial delamination occurs, and then reaches the fracture strain of 49%.

4. DISCUSSION

In the as-twin-roll-cast Ti/Al clad sheet (AS sheet), the solidified microstructure in the Al alloy substrate side is relatively homogeneous, and reaction products are not formed at the Ti/Al interface (Fig. 2(b)) because the diffusion bonding time may not be sufficient during the twin roll casting, which results in the poor strength and ductility (Table 1). This as-twin-roll-cast sheet should be annealed to recover properties of cast Al alloy substrate and to improve the interfacial bonding [36,37]. After the stress-relief annealing at 400 °C for 10 min (A41 sheet), the metallurgical bonding is expanded by the interfacial diffusion, although it is not clearly visible in the Ti/Al interface, thereby leading to the improvement in tensile properties (Table 1). When the annealing time increases to 30 min (A43 sheet), tensile properties are more improved as the interfacial bonding increases.

When the AS sheet is annealed at higher temperatures, *e.g.*, 600 °C, a reaction phase of $TiAl_3$ intermetallic compound is formed at the Ti/Al interface, as shown in Figs. 3(d) and 4(a). This interfacial $TiAl_3$ generally helps to improve the interfacial bonding, but often deteriorates tensile or interfacial bonding properties because it has inherently brittle characteristics [13,38,39], although trends of increased tensile and interfacial bonding are generally accepted at a certain thickness level of interfacial layer [13]. After the annealing at 600 °C for 10 min, tensile properties are slightly better than those of the A43 sheet. This is closely related with the formation of interfacial $TiAl_3$ (Fig. 3(c)), and indicates that this $TiAl_3$ phase improves tensile properties when it is optimally controlled. In the A63 sheet, however, the interfacial layer is grown to 2.9 μm, thereby resulting in the decrease in tensile properties. This is because the interfacial layer is thickened over a certain optimal thickness level, *e.g.*, 1.2 μm.

The interfacial layer in the A61 sheet favorably affects tensile properties as well as interfacial bonding, but is relatively easily cracked to induce an interfacial delamination during the tensile test which is closely related with a rapid

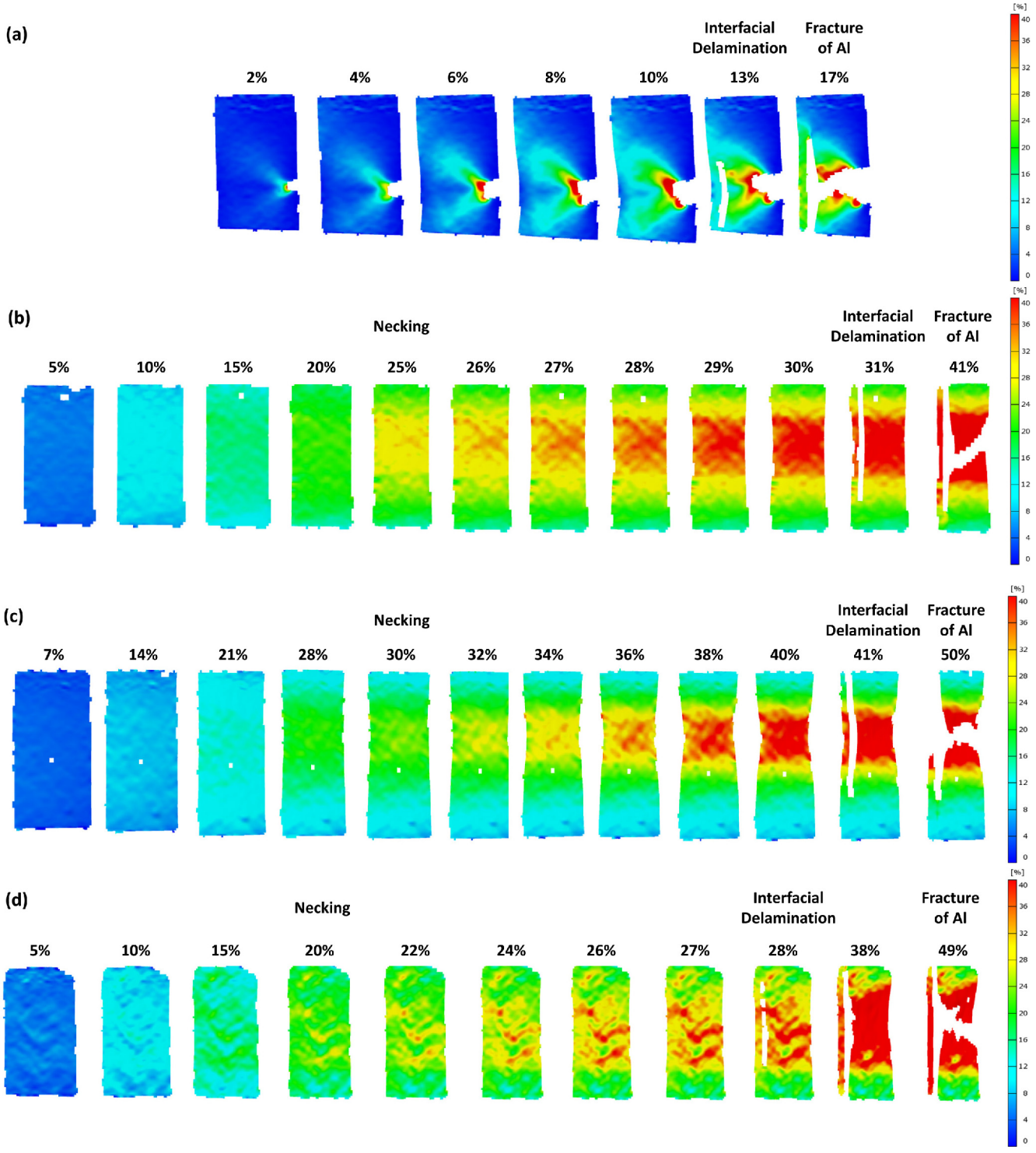

Fig. 6. Digital images of strain distribution of the tensioned (a) AS, (b) A41, (c) A43, and (d) A61 sheets. The Ti/Al interface is delaminated after the necking, which leads to the rapid stress drop in the stress-strain curve (Figures 5(a) through (c)).

stress drop in the stress-strain curve (Fig. 5(c)). According to the DIC results of the tensioned A61 sheet (Fig. 6(d)), the homogeneous deformation occurs while the strain increases continuously to 15%, and the necking and interfacial delamination appear at the strain of 20% and 28%, respectively. Though the A61 sheet is continuously deformed further until the fracture strain of 49%, the additional ductility after the interfacial delamination has no meaning in the tensile property evaluation because the delaminated clad sheets are not useful any more. Considering that the strain at the interfacial

delamination point is more meaningful in the property evaluation of the Ti/Al clad sheets than the fracture strain, the A43 sheet shows the best tensile properties among the Ti/Al clad sheets as the A61 sheet shows the lower delamination strain than the A43 sheet (41% *vs* 28%).

Since the Ti/Al interface is well bonded without any defects, the yield and tensile strengths can be simply calculated by a rule of mixtures. The yield and tensile strengths of the A43 sheet (132 MPa and 218 MPa, respectively) are higher than those (103.3 MPa and 202.5 MPa, respectively) calculated from basic tensile properties of a 5052-O Al alloy (thickness; 2.5 mm, 90 MPa and 195 MPa, respectively) and a pure Ti (675 °C-annealed, thickness; 0.5 mm, 170 MPa and 240 MPa, respectively). This result indicates that the A43 sheet shows higher yield and tensile strengths than the calculated strengths. In addition, the ductility of the A43 sheet is higher than that of the 5052-O Al alloy (25%) [40] or the pure Ti (25%) [41] because its strain at the interfacial delamination reaches 41%. The A43 sheet shows the overall homogenous deformation behavior (Fig. 6(c)) by complimenting drawbacks of mono-layer Al or Ti sheet, while fully taking advantage of each sheet.

The present application of twin-roll casting and stress-relief annealing would prove a good way to successfully fabricate Ti/Al clad sheets having excellent tensile properties. It is also useful to understand the interfacial bonding behavior and to suggest optimal annealing conditions. The as-twin-roll-cast Ti/Al clad sheet inevitably contains a weak interface because of insufficient diffusion bonding, but the interfacial bonding and tensile properties are dramatically improved after the stress-relief annealing. Since the stress-relief annealing is actually involved in commercial fabrication processes of 5052 Al alloy sheets, any additional processing equipments are not needed. The present twin-roll-cast Ti/Al clad sheets have excellent tensile properties and economic advantages as well, and thus present new applications to multi-functional lightweight metal alloy sheets requiring excellent corrosion resistance, formability, and alloy cost saving as well as mechanical properties. In addition, the tensile deformation and interfacial debonding behavior can be well interpreted by the DIC technique, *i.e.*, macroscopic local strain distribution analyses. The DIC technique is an excellent method for detailed analyses of tensile tests of the Ti/Al clad sheets, and can also provide an important idea for practical ductility analyses.

5. CONCLUSION

A new fabrication method of Ti/Al clad sheets by bonding a thin Ti sheet on to Al alloy melt during twin-roll casting was presented in this study.

(1) In the as-twin-roll-cast Ti/Al clad sheet, the homogeneously solidified microstructure existed in the cast Al alloy substrate side, while wrinkles were not formed in the Ti alloy side. The Ti/Al interface was clearly observed, but did not contain any pores, cracks, or lateral delamination, which indicated the successful fabrication of the Ti/Al clad sheet without any cast or interfacial defects.

(2) The as-twin-roll-cast sheet was stress-relief-annealed to recover properties of cast Al alloy substrate and to improve the interfacial bonding. After the annealing at 400 °C for 10 min, the metallurgical bonding was expanded by the interfacial diffusion, although it was not clearly visible in the Ti/Al interface, thereby leading to the improvement in tensile properties. When the annealing time increased to 30 min, tensile properties were more improved as the interfacial bonding increased.

(3) When the as-twin-roll-cast sheet was annealed at 600 °C, a reaction phase of $TiAl_3$ intermetallic compound was formed at the Ti/Al interface. Since this interfacial $TiAl_3$ helped to improve the interfacial bonding, tensile properties of the 600 °C-10-min-annealed sheet were slightly better than those of the 400 °C-annealed sheets. In the 600 °C-30-min-annealed sheet, however, the interfacial layer was grown to 2.9 μm, thereby resulting in the decrease in tensile properties because of brittle characteristics of too thickened interfacial layer.

4) According to the digital image correlation results of the 600 °C-10-min-annealed sheet, the homogeneous deformation occurred while the strain increased continuously to 15%, and the necking and interfacial delamination appeared at the strain of 20% and 28%, respectively. Considering that the strain at the interfacial delamination point was more meaningful in the property evaluation of the Ti/Al clad sheets than the fracture strain, the 400 °C-30-min-annealed sheet showed the higher delamination strain than the 600 °C-10-min-annealed sheet (41% *vs* 28%).

5) The yield and tensile strengths of the 400 °C-30-min-annealed sheet (132 MPa and 218 MPa, respectively) were higher than those (103 MPa and 203 MPa, respectively) calculated by a rule of mixtures using tensile properties of a 5052-O Al alloy and a pure Ti. Its ductility was also higher than that of 5052-O Al alloy (25%) or pure Ti (25%) because the delamination strain reached 41%. The 400 °C-30-min-annealed sheet showed the overall homogenous deformation behavior by complimenting drawbacks of mono-layer Al or Ti sheet, while fully taking advantage of each sheet.

ACKNOWLEDGMENT

This study was supported by the Fundamental R&D Program for Core Technology of Materials of the Ministry of Knowledge Economy, Korea (grant number 10037273), POSCO (grant number 2014Y008), and Brain Korea 21 PLUS Project for Center for Creative Industrial Materials.

REFERENCES

1. S. J. Li, M. T. Jia, F. Prima, Y. H. Hao, and R. Yang, *Scripta Mater.* **64**, 1015 (2011).

2. S. B. Gabriel, J. V. P. Panaino, I. D. Santos, L. S. Araujo, P. R. Mei, L. H. de Almeida, *et al. J. Alloy. Compd.* **536**, S208 (2012).
3. J. M. Oh, J. W. Lim, B. G. Lee, C. Y. Suh, S. W. Cho, G. S. Choi, *et al. Mater. Trans.* **51**, 2009 (2010).
4. J. M. Calderon Moreno, M. Popa, S. Ivanescu, C. V. S. I. Drob, E. I. Neacsu, and M. V. Popa, *Met. Mater. Int*. **20**, 177 (2014).
5. R. R. Boyer, *Mat. Sci. Eng. A* **213**, 103 (1996).
6. H. Nan and C. M. Xie, *China Foundry Machinery & Technol*. **6**, 1 (2003).
7. Y. Zhou, X. J. Yang, and Z. D. Cui, *Met. Sci. Heat Treat*. **1**, 47 (2005).
8. I. V. Gorynin, *Mat. Sci. Eng. A* **263**, 112 (1999).
9. L. Peng, J. Wang, H. Li, J. Zhao, and L. He, *Scripta Mater.* **52**, 243 (2005).
10. J. Baird, *J. Nucl. Energy A* **11**, 81 (1960).
11. J. Liu, Y. Su, Y. Xu, L. Luo, J. Guo, and H. Fu, *Rare Metal. Mat. Eng.* **40**, 753 (2011).
12. J.-P. Liu, L.-S. Luo, Y.-Q. Su, Y.-J. Xu, X.-Z. Li, R.-R. Chen, *et al. T. Nonferr. Metal. Soc*. **21**, 598 (2011).
13. Y. Wei, W. Aiping, Z. Guisheng, and R. Jialie, *Mat. Sci. Eng. A* **480**, 456 (2008).
14. L. Xu, Y. Y. Cui, Y. L. Hao, and R. Yang, *Mat. Sci. Eng. A* **435-436**, 638 (2006).
15. J. Oh, W. Lee, S. G. Pyo, W. Park, S. Lee, and N. J. Kim, *Metall. Mater. Trans. A* **33**, 3649 (2002).
16. Y.-B. Sun, Y.-Q. Zhao, D. Zhang, C.-Y. Liu, H.-Y. Diao, and C.-L. Ma, *T. Nonferr. Metal. Soc.* **21**, 1722 (2011).
17. M. Simsir, L. C. Kumruoğlu, and A. Özer, *Mater. Design*. **30**, 264 (2009).
18. K. Shibuya and M. Ozawa, *ISIJ Int.* **31**, 661 (1991).
19. T. Haga and S. Suzuki, *J. Mater. Process. Tech.* **137**, 92 (2003).
20. T. Haga, K. Tkahashi, M. Ikawaand, and H. Watatari, *J. Mater. Process. Tech.* **153-154**, 42 (2004).
21. D. Liang and C. B. Cowley, *JOM* **56**, 26 (2004).
22. T. Haga, H. Watari, and S. Kumai, *J. Achi. Mater. Manu. Eng.* **15**, 186 (2006).
23. S. S. Park, W. J. Park, C. H. Kim, and N. J. Kim, *JOM* **61**, 14 (2009).
24. J. K. OH, S. G. Pyo, S. Lee, and N. J. Kim, *J. Mater. Sci*, **38**, 3647 (2003).
25. L. Wang, H. Yu, Y, Lee, and H.-W. Kim, *Met. Mater. Int.* **21**, 832 (2015).
26. D.-H. Koh, Y.-S. Lee, M.-S. Kim, H.-W. Kim, and Y.-S. Ahn, *Korean J. Met. Mater*. **54**, 483 (2016).
27. D. Goda, N. Richards, W. Caley, and M. Chaturvedi, *Mat. Sci. Eng. A* **334**, 280 (2000).
28. M. Mirjalili, M. Soltanieh, K. Matsuura, and M. Ohno, *Intermetallics* **32**, 297 (2013).
29. M. J. Kim, G.-Y. Kim, K. J. Euh, Y.-M. Rhyim, and K.-A. Lee, *Korean J. Met. Mater.* **53**, 169 (2015).
30. K. R. Van Horn, *Aluminum,* Vol. 3, p. 327, American Society for Metals, Ohio, USA (1967).
31. ASTM E8/E8M, *Standard Test Methods for Tension Testing of Metallic Materials*, Vol. 03.01, Annual Book of ASTM Standards (2007).
32. B. Wattrisse, A. Chrysochoosm J.-M. Muracciole, and M. Némoz-Gaillard, *Exp. Mech.* **41**, 29 (2001).
33. J. Kang, Y. Ososkov, J. D. Embury, and D. S. Wilkinson, *Scripta Mater.* **56**, 999 (2007).
34. W. J. Parker, R. J. Jenkins, C. P. Butler, and G. L. Abbott, *J. Appl. Phys.* **32**, 1679 (1961).
35. Y. Mishin and C. Herzig, *Acta Mater.* **48**, 589 (2000).
36. G. Shi and J. Qiao, *Adv. Mat. Res.* **239**, 50 (2011).
37. Y. Wang, S. B. Kang, and J. Cho, *J. Alloy. Compd.* **509**, 704 (2011).
38. K. S. Lee, J. -S. Kim, Y. M. Jo, S. E. Lee, J. Heo, Y. W. Chang, *et al. Mater. Charact.* **75**, 138 (2013).
39. J. S. Kim, K. S. Lee, Y. N. Kwon, B.-J. Lee, Y. W. Chang, and S. Lee, *Mat. Sci. Eng. A* **628**, 1 (2015).
40. K. R. Van Horn, *Aluminum,* Vol. 1, p. 314, American Society for Metals, Ohio, USA (1967).
41. I. J. Polmear, *Light Alloys Metallurgy of the Light Metals, 3rd ed*., p. 250, Arnold, London, UK (1995).